

Maderas-Cienc Tecnol 22(s/n):2020  
Ahead of Print: Accepted Authors Version

DOI:10.4067/S0718-221X2020005XXXXXX

1  
2 **INFLUENCE OF NANO WOLLASTONITE ON PHYSICAL,**  
3 **MECHANICAL AND MORPHOLOGICAL PROPERTIES OF GYPSUM**  
4 **COMPOSITES MANUFACTURED FROM BAGASSE**

5 **Ali Hassanpoor Tichi<sup>1,\*</sup>, Habibollah Khademislam<sup>2</sup>, Mojtaba Rezanezhad Divkolae<sup>1</sup>**

6 <sup>1</sup>Department of Wood Science and Engineering, Technical Faculty of Number 2 (Shahid  
7 Hasheminejad), Mazandaran Branch, Technical and Vocational University (TVU), Sari, Iran.

8 <sup>2</sup>Department of Wood and Paper Science and Technology, Faculty of Agriculture and Natural  
9 Resources, Science and Research Branch, Islamic Azad University, Tehran, Iran.

10 **^Corresponding author:** [hasanpoortichi@gmail.com](mailto:hasanpoortichi@gmail.com)

11 **Received:** October 26, 2019

12 **Accepted:** April 30, 2020

13 **Posted online:** April 30, 2020

14 **ABSTRACT**

15 We investigated the effect of adding nano-wollastonite on the physical, mechanical and  
16 morphological properties of gypsum Composites. The ratio percentage of bagasse mixing as  
17 lignocellulosic material with gypsum at three levels (85:15; 75:25; 65:35) and nano-wollastonite  
18 at three levels of 0 %, 5 % and 10 %. Specimens were prepared according to the ISO 11925  
19 specifications for the fire resistance (weight loss) properties and according to the DIN EN 634-1:  
20 1195-04 specifications for the mechanical and physical properties. Scanning Electron  
21 Microscopy (SEM) were also used to study the properties of composite morphology and  
22 distribution of samples. The results showed that by increasing the amount of nano wollastonite,  
23 physical and mechanical properties improved. The MOR, MOE and IB of boards decreased with  
24 increased bagasse usage amount, and its maximum value was obtained in using 15 % bagasse.  
25 The results also showed that increasing the amount of bagasse in boards caused a significant  
26 increase in the TS of the boards. The results from microscopic images showed that the optimal  
27 level of nano-wollastonite can fill the empty holes and create a uniform structure, thereby  
28 improving the properties of the boards.

29 **Keywords:** Bagasse, internal bonding, density, Modulus of rupture, nano wollastonite

30  
31  
32  
33  
34  
35

## INTRODUCTION

36  
37  
38  
39  
40  
41  
42  
43  
44  
45  
46  
47  
48  
49  
50  
51  
52  
53  
54  
55  
56  
57  
58

Gypsum board is an inorganic-bonded panel produced from wood chip and agricultural waste (bagasse) using gypsum as adhesive. It has been primarily used for residential construction, such as wall and roof sheathing. A good building construction material, gypsum board does not emit formaldehyde and also has features high resistance to fire (Deng and Furuno 2001).

Properties of gypsum particleboard reinforced with polypropylene fibers showed that the addition of PP fibers reduced the IB, MOR, MOE and increased the thickness swelling of gypsum board (Deng and Furuno 2001). The physical and mechanical properties of gypsum particleboard reinforced with Portland cement have been examined by Espinoza-Herrera and Cloutier (2011). The results showed that Portland cement incorporation increased the mechanical resistance of the boards.

Agricultural waste that can be used in the gypsum board industry includes rice straw, sunflower stem and bagasse. All of these materials, such as giant reed (*Arundo donax*), can be used produce different types of composite materials. However, these materials have some negative effects on the properties of composites. Due to high concentration of extractives compared to wood materials, higher inhibitory effects of available extractives in non-wood materials or agricultural residues can be expected on the hydration process of cement paste. Presence of these compounds increases the proportion of un-hydrated cement particles and decreases the strength of the cement-bonded particle board (Wei *et al.* 2003).

It is also possible to increase the reaction speed between gypsum and lignocellulosic material and to reduce the negative effect of extractives by using additives such as calcium chloride and inorganic nanomaterials such as nano-silica and nano-wollastonite. In this study, we used nano-wollastonite to further adapt gypsum to lignocellulosic material. There have been many studies

59 around the world of the effect of nano-wollastonite on wood and composite products, but the  
60 effect of nano-wollastonite on gypsum has not been investigated.

61

62 Commercial grades of wollastonite are typically high in purity. This is due to the fact that almost  
63 all manufacturers use wet processing, high-intensity magnetic separation, and/or heavy media  
64 separation to remove accessory minerals (Ciullo 1997). The minerals most commonly found  
65 associated with wollastonite are calcite (calcium carbonate), diopside (calcium magnesium  
66 silicate), and garnet (calcium aluminum silicate). Wollastonite is hard, white, and alkaline with a  
67 pH of 8+/-1. It is exploited for its chemistry as a source of CaO and SiO<sub>2</sub>, and its low loss on  
68 ignition (LOI– Determining the total volatile content), low oil absorption, low moisture  
69 absorption, and fire-retarding properties (Ciullo 1997). The effect of wollastonite has been  
70 reported to improve the dimensional stability of solid woods (Poshtiri *et al.* 2013), and to  
71 increase the thermal conductivity coefficient of medium-density fiberboards (MDF) (Taghiyari *et*  
72 *al.* 2013). Fire-retardant properties of wollastonite have been noted in the literature when it is  
73 used in solid wood and wood composite materials (Poshtiri *et al.* 2013, Taghiyari *et al.* 2013).  
74 Khosrviyan (2009) reported that the physical and mechanical properties of wood-plastic  
75 composite were improved with the addition of wollastonite.

76 Yel *et al.* (2020) have reported a relationship between press temperatures of (20, 30, 40, 50, 60,  
77 70 and 80) °C on physical, mechanical and thermal properties of cement-bonded particleboard  
78 made from the particles of spruce (*Picea orientalis*) and poplar (*Populus tremula*). According to  
79 their results, the most mechanical and physical resistance of boards were found as 40 °C for  
80 poplar wood and 60 °C for spruce wood.

81 Papadopoulos (2008), described that the cement bonded particleboards was resistant to fungi  
82 (brown and white rot). fungi failed to attack the cement-bonded boards.

83 The aim of this research was to study the physical and mechanical properties of a gypsum board.  
84 Hence, the effect of using bagasse (15 %, 25 %, or 35 %, with respect to the total content of  
85 binder in each mixture), as the replacement of the wood in gypsum system, and also of adding  
86  $\text{CaSiO}_3$ , as additive at nano wollastonite (0 %, 5 % or 10 %, dry weight basis of cement ) to the  
87 complex of bagasse-gypsum, on the physical and mechanical behavior of gypsum and properties  
88 of the gypsum were examined.

## 89 MATERIALS AND METHODS

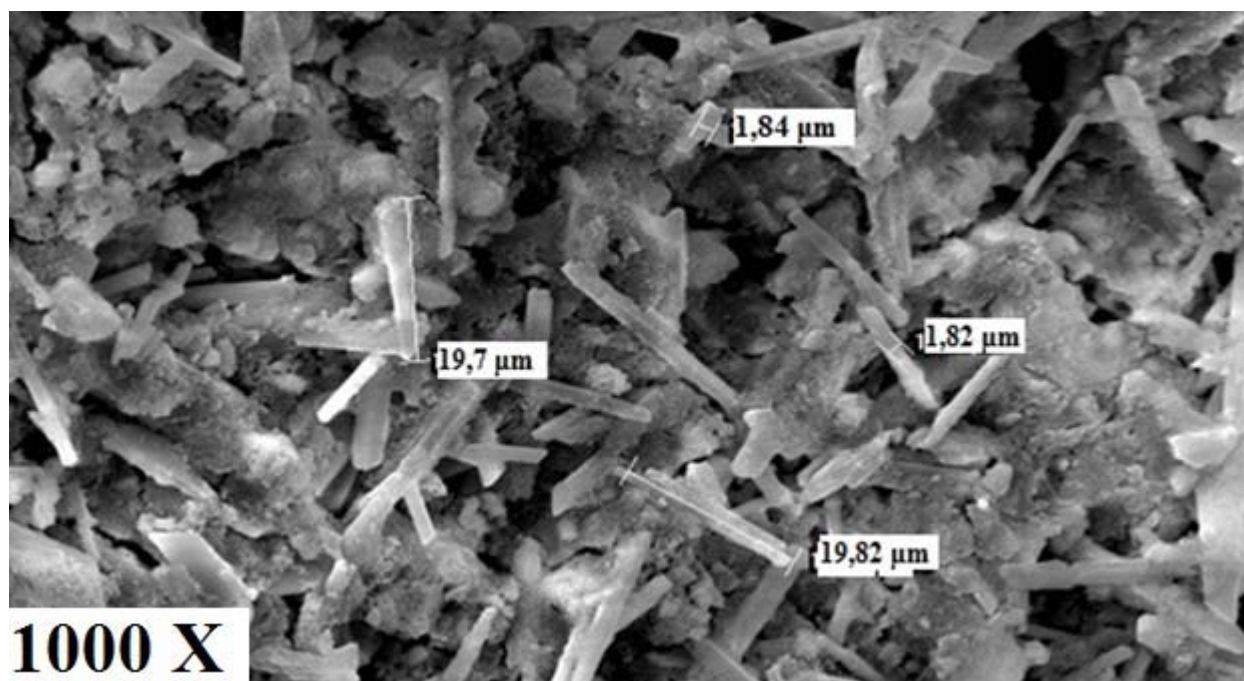
### 90 Specimen Procurement

91 The natural gypsum used in this research was purchased from Omid Company (Semnan, Iran).  
92 Agricultural waste used in this research was bagasse obtained from Sugar cane workshop  
93 (Bahnemir, Iran). Chemical composition of bagasse was in table 1. Commercial wollastonite was  
94 purchased from Vard manufacturing company of mineral and industrial products (Tehran, Iran).  
95 Dimensions of the nano wollastonite and specifications of the wollastonite composition are given  
96 in Figure 1 and table 2, respectively. Density wollastonite was  $2,92 \text{ g/cm}^3$ .

97 **Table 1:** Chemical composition of bagasse.

Chemical Compounds	Percentage (%)
Cellulose	47,6
Lignin	23,2
Ash	1,7
Extractives	4,1
Silica	0,9
Silica in ash	42,9

98



99

100

101

102

**Figure 1:** SEM micrograph of nano wollastonite.

**Table 2:** Composition of the Wollastonite Gel.

Inorganic component	Percentage (%)
SiO <sub>2</sub>	46,96
CaO	39,77
Fe <sub>2</sub> O <sub>3</sub>	2,79
Al <sub>2</sub> O <sub>3</sub>	3,95
TiO <sub>2</sub>	0,22
K <sub>2</sub> O	0,04
MgO	1,39
Na <sub>2</sub> O	0,16
SO <sub>3</sub>	0,05
Water	4,67

103

104 Bagasse (Figure 2A) were applied at three proportions (15 %, 25 %, or 35 %, with respect to the  
105 total content of binder in each mixture and different wollastonite substitution levels 0 %, 5 % or  
106 10 %) for gypsum. The moisture content of bagasse was 50 % before dryer and 6 % after dryer,  
107 also oven dry density bagasse was 0,39 g/cm<sup>3</sup>.

### 108 **Composite panel production**

109 First, bagasse was washed hot water and then milled into particles using a hammer mill (Figure  
110 2A). Particle size average was 2 cm to 3 cm length 1 mm to 2 mm thickness. Oven dry density  
111 and dimensions of all boards were set at 1,1 g/cm<sup>3</sup> 550 × 270 × 20 mm<sup>3</sup>. Therefore, for the  
112 production of boards, the density (oven dry) of raw materials in each treatment was calculated  
113 first using density formula. Then the weight ratios of each board were determined (Table 3).  
114 Next, using a digital scale, the ratios of water, nano-wollastonite and calcium chloride were  
115 determined, and after mixing them in the mixing apparatus (laboratory mixer), these materials  
116 were added to the bagasse and gypsum paste that had already been weighted. Subsequently, the  
117 cake from the mixing machine was poured uniformly into a 55 × 27 × 6 cm<sup>3</sup> metal mold and  
118 pressed under pressure (Burkle-LA-160) under cold (room conditions for 10 minutes at a  
119 pressure of 30 kg/cm<sup>2</sup> to reach final thickness 20 mm). After pressing, the boards were kept for  
120 24 hours conditions (20 °C ± 1 °C, 65 % ± 2% RH). After initial cooling, the boards were kept in  
121 a special chamber at a temperature of about 20 °C and relative humidity above 90 % for 20 days  
122 in order to minimize drying speed. After that, the boards were removed using a circular saw and  
123 placed in an air-conditioned room at 20 °C and 65 % relative humidity for 28 days (Figure 2B).



**Figure 2:** Bagasse chip (A), Gypsum board with bagasse chip (B).

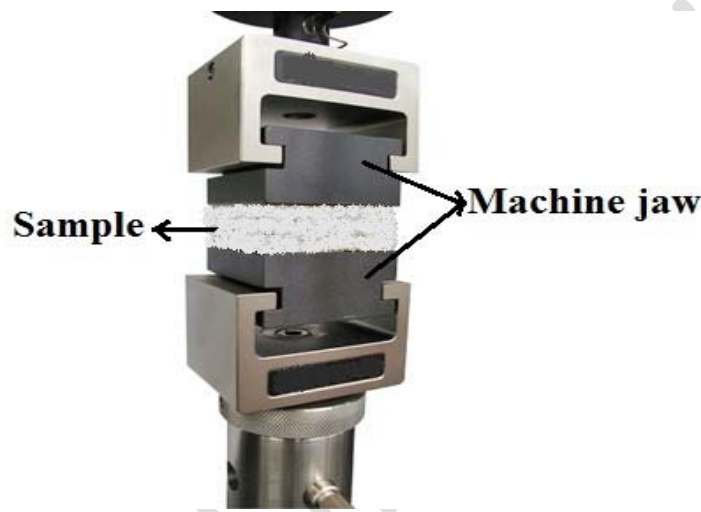
**Table 3:** Weight ratios of each board.

Nano-wollastonite (%)	Gypsum- bagasse (%)	Bagasse weight (g)	Gypsum weight (g)	Nano wollastonite weight (g)	Total weight (g)
0 %	85 % -15 %	445,5	2524,5	-	2970
	75 % -25 %	742,5	2227,5	-	2970
	65 % -35 %	1039,5	1930,5	-	2970
5 %	85 % -15 %	445,5	2398,28	126,22	2970
	75 % -25 %	742,5	2116,125	111,375	2970
	65 % -35 %	1039,5	1833,975	96,525	2970
10 %	85 % -15 %	445,5	2272,05	252,45	2970
	75 % -25 %	742,5	2004,75	222,75	2970
	65 % -35 %	1039,5	1737,45	193,05	2970

### Mechanical and Physical Tests

The samples were then evaluated for static bending three points edgewise such as modulus of rupture (MOR), modulus of elasticity (MOE) and internal bonding (IB) according to DIN EN 634-1:1195-04 (DIN 1995) using a universal testing machine (model GT-TCS-2000; Taichung Industry Park, Taichung, Taiwan) at the speed of 10 mm/min. Three replicates were made at a dimension of  $550 \times 270 \times 20 \text{ mm}^3$  for each board type. Samples dimensions for static bending and internal bonding test were 450 (loading span: 400 mm) length  $\times$  50 width  $\times$  20 thickness

136 (mm<sup>3</sup>) and 50 length × 50 width × 20 thickness (mm<sup>3</sup>), respectively. For IB test, first, cut the  
137 specimens to 5 cm × 5 cm dimensions and then we glue them to the special jaws of the machine.  
138 Next we place the jaws inside the machine. The apparatus applies tensile force to the jaws,  
139 causing fractures in the specimen's brain, resulting in the amount of internal bonding being  
140 determined (Figure 3).



141  
142 **Figure 3:** Testing machine for internal banding.

143 The load and deflection were continuously recorded and the data were used to calculate modulus  
144 of rupture (MOR), modulus of elasticity (MOE) and internal bonding (IB) in based on equations.  
145 1, 2 and 3:

146 
$$MOR = 1,5 \frac{PL}{bd^2} \quad (1)$$

147 
$$MOE = \frac{PL^3}{4bd^3D} \quad (2)$$

148 
$$IB = \frac{P_{max}}{A} \quad (3)$$

149  
150 Where  $P$  is the maximum force (N),  $L$  is the span length (mm),  $b$  is the sample width (mm),  $d$  is  
151 the sample thickness (mm),  $D$  is the deflection,  $A$  is the felling area (mm<sup>2</sup>).

152



153 **Physical tests**

154 The effect of composite formulation on the thickness swelling after 2 and 24 hours immersion in  
155 water was determined in samples with the dimensions of 50 mm × 50 mm × 20 mm according to  
156 DIN EN 634-1:1195-04 (DIN 1995). Sample was soaked in distilled water for 2 h and 24 h  
157 (room temperature). TS were then calculated according to the following equations:

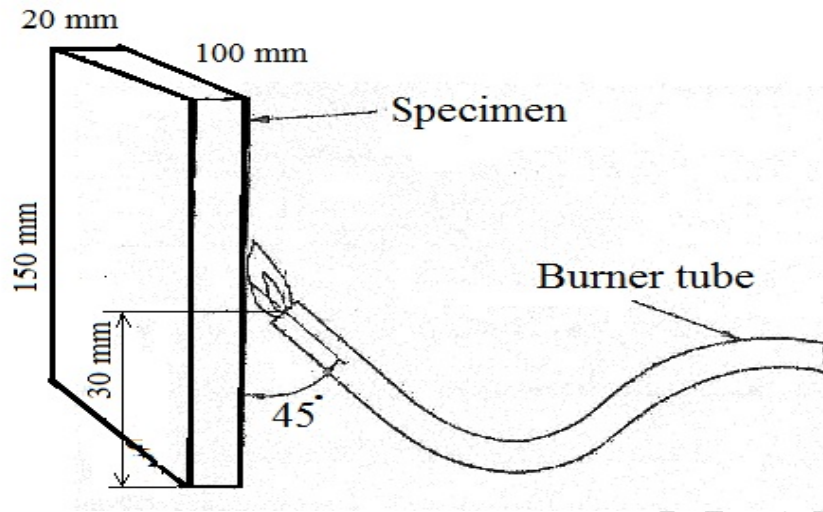
158 
$$TS = \frac{T_2 - T_1}{T_1} \times 100 \quad (4)$$

159 where TS is thickness swelling (%),  $T_1$  is thickness before immersing,  $T_2$  is thickness after each  
160 immersion.

161 **Fire-Retardant Testing Apparatus**

162 The boards measuring 150 length × 100 width × 20 thickness ( $\text{mm}^3$ ) were prepared according to  
163 the ISO 11925 (ISO 2010) specifications for the fire resistance tests (figure 4). Mass loss of the  
164 samples due to fire exposure was vertically mounted on a holder up-straight and exposed to a  
165 Bunsen-type burner (with the internal diameter of 11 mm) hold at 45 degrees to the surface of  
166 the specimen for 120 seconds in accordance with method described by Esmailpour *et al.* (2017).  
167 Then, the burnt area, as well as weight loss, is measured. From the preliminary weight of  
168 specimens before fire exposure ( $W_1$ ) and second weight of specimens after fire exposure ( $W_2$ ),  
169 the Mass loss (ML) was calculated as follows:

170  
171 
$$ML (\%) = \{(W_2 - W_1) / W_1\} \times 100 \quad (5)$$



172  
173 **Figure 4:** Schematic picture of fixed fire testing apparatus.

174 **Scanning Electron Microscopy (SEM)**

175 The fracture surfaces were analyzed from samples fractured in the flexural strength test, using  
176 images obtained by scanning electron microscopy. The maximum magnification used here was  
177 3000x. The specimens were cut with dimensions of 10 mm × 10 mm, attached to a sample holder  
178 and metallized with gold. The microscope used here was a Philips model XL 30 FEG carried out  
179 at the School of Electrical and Computer Engineering, University of Amir Kabir, Tehran, Iran.

180 **Statistical analyses**

181 Statistical analyses were performed using Statistica software v.13 (Dell Inc. 2016). The obtained  
182 results were analyzed statistically, and an analysis of variance (ANOVA) was performed to  
183 determine the significance of the tested parameter. A duncan's multiple range test (DMRT) was  
184 performed to compare treatment means.

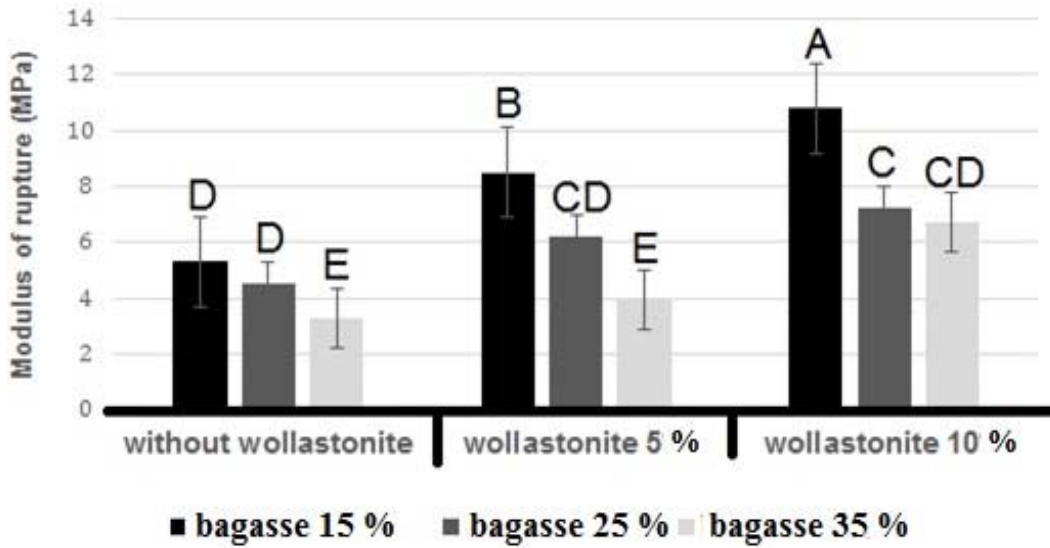
185  
186  
187

## RESULTS AND DISCUSSION

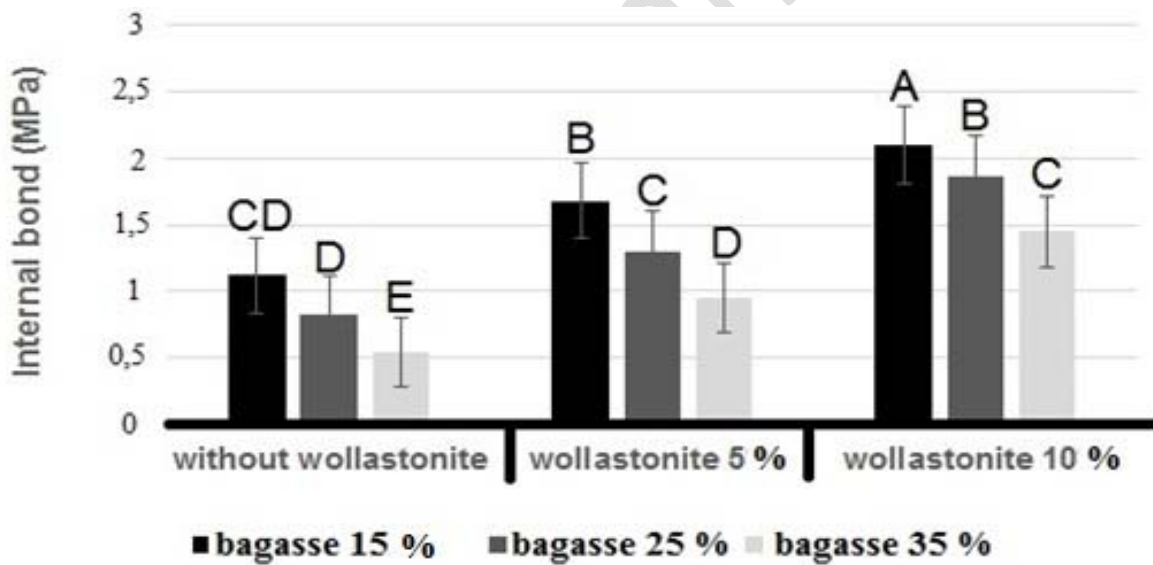
188  
189  
190  
191  
192  
193  
194  
195  
196  
197  
198  
199  
200  
201  
202  
203  
204  
205  
206  
207  
208  
209  
210  
211

### **Mechanical properties of the gypsum boards**

The results from the mechanical testing are shown in Figure 5, 6 and 7. As shown, the MOR, MOE and IB values increased in the gypsum boards that contained wollastonite compared to the gypsum boards without wollastonite. The highest and lowest modulus of rupture (MOR), values were found in the 10 % wollastonite and 15 % bagasse chip (10,8 MPa) and 0 % wollastonite and 35 % bagasse chip (3,25 MPa) treatments, respectively (Figure 5). Results of the modulus of elasticity (MOE) tests indicated that the highest (4870 MPa) and lowest (2370 MPa) MOE values were found in the same treatments as the highest and lowest MOR values (Figure 6). The highest and lowest internal bond (IB) values were found in the 10 % wollastonite and 15 % bagasse chip (2,1 MPa) and 0 % wollastonite and 35 % bagasse chip (0,54 MPa) boards, respectively (Figure 7). The abundance of extractive materials in lignocellulosic materials and agricultural wastes, especially phenolic and sugary materials, reduces gypsum hydration heat, slows the hydration reaction time, and increases bagasse retention time (Rangavar *et al.* 2016). There are several reasons for the increased mechanical properties with increasing nano-wollastonite in the mix. By measuring the hydration heat of gypsum-bagasse slurry and different amounts of nano-wollastonite, it was found that with increasing nano, the hydration heat was increased, which resulted in faster and better curing of bagasse with gypsum and thus increased board strength. Silica in nano-wollastonite forms a calcium silicate hydrate (Ca-Si-H) gel, preventing the penetration of chlorine ions, sulfates and other harmful chemicals into boards, increasing durability, increasing hydration heat, speeding gypsum and mechanical strength (Li *et al.* 2004). High substitution levels of wollastonite mitigated the negative effect of the extractive materials (Karimi *et al.* 2012; Ma and Wang 2012). Consequently, the mechanical properties were improved.

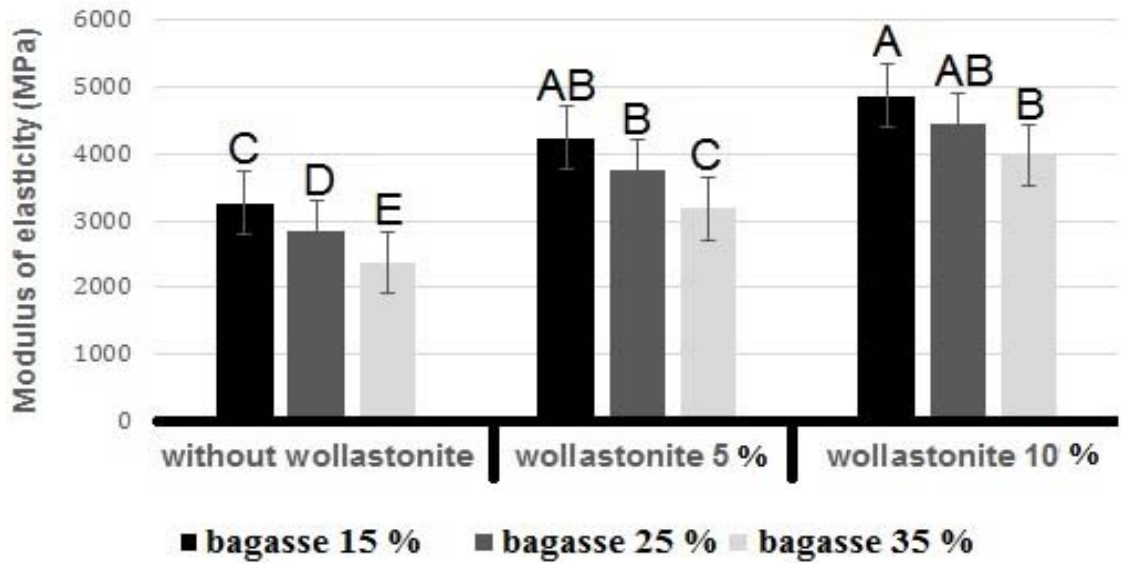


212 **Figure 5:** Effect of varying levels of nano wollastonite on the MOR of composites composed of  
213 different percentages of bagasse; letters on each column indicate Duncan's grouping at the 99 %  
214 level of confidence.



215 **Figure 6:** Effect of varying levels of nano wollastonite on the MOE of composites composed of  
216 different percentages of bagasse; letters on each column indicate duncan's grouping at the 99 %  
217 level of confidence.

218  
219  
220  
221



222 **Figure 7:** Effect of varying levels of nano wollastonite on the IB of composites composed of  
223 different percentages of bagasse; letters on each column indicate duncan's grouping at the 99 %  
224 level of confidence.

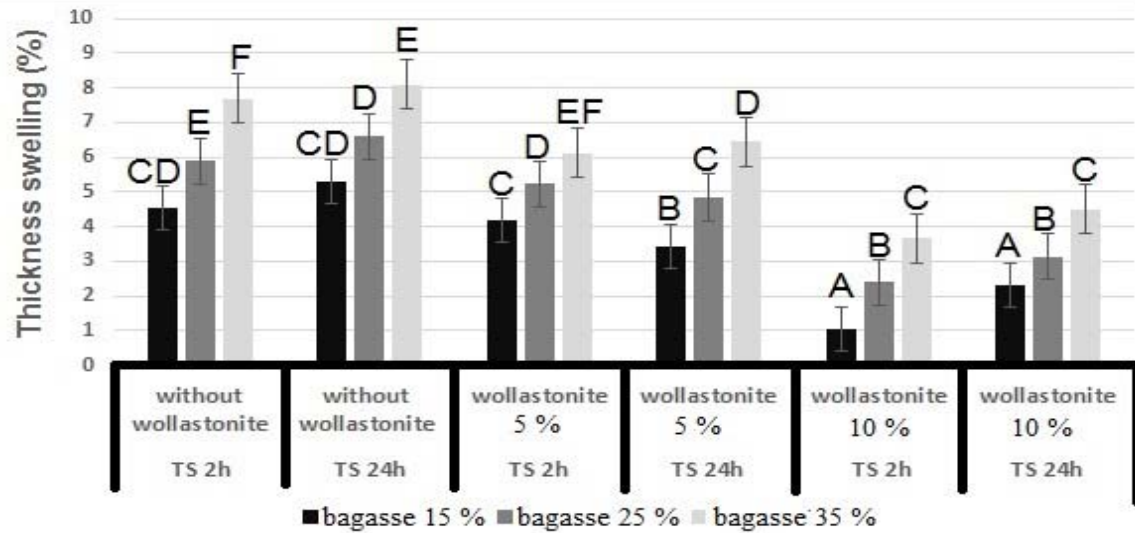
#### 225 **Physical properties of the gypsum boards**

226 The physical properties of the panels evaluated were thickness swelling after 2 and 24 hours  
227 immersion in water, density and fire resistance (Mass loss). The results of these tests are  
228 presented in the Figure 8, 9 and 10. Adding nano wollastonite to gypsum board has been shown  
229 to decrease the thickness swelling of boards. The lowest thickness swelling was observed for 10  
230 % wollastonite and 15 % bagasse chip, and the highest was observed for the sample without  
231 wollastonite and 35 % bagasse chip (Figure 8). Nano-wollastonite addition to gypsum board and  
232 increases the density and decreases the air content in boards. The highest density was found in 10  
233 % wollastonite and 15 % bagasse chip, showing 28 % of increase in comparison to the sample  
234 without wollastonite and 35 % bagasse chip (Figure 9). One of the reasons can be attributed to  
235 biometrics, slimming coefficient, sponge structure and hydrophilic properties of bagasse. It was  
236 also observed that with increasing nano, the dimensional stability of the boards improved. The  
237 reason for this can be attributed to the hydrophobicity of nano-wollastonite (Ciullo 1997). Nano-

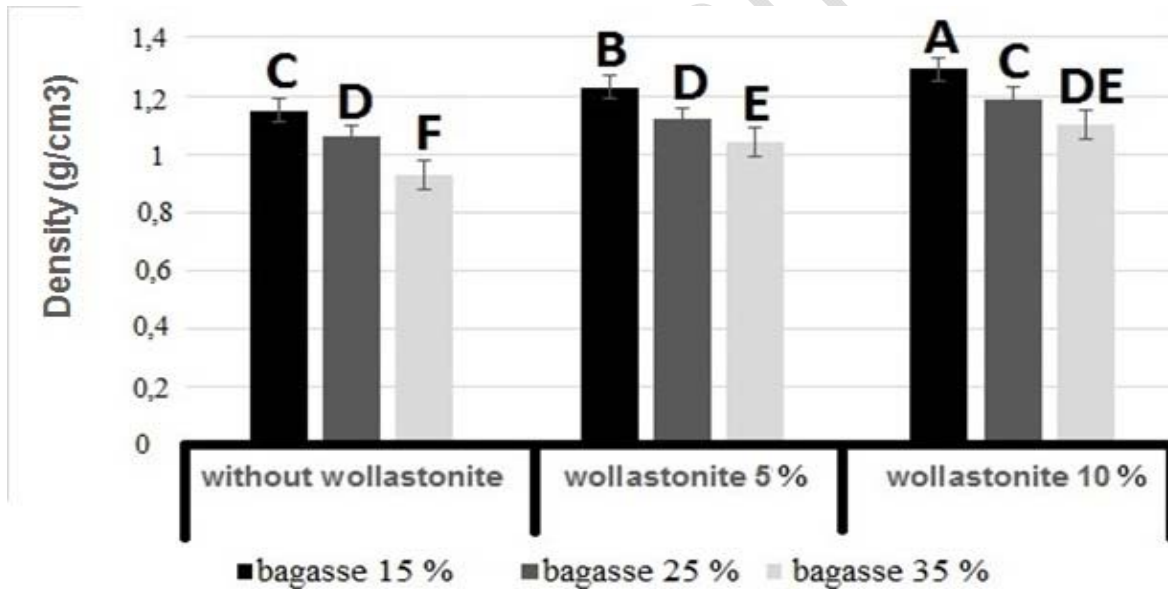
238 wollastonite, due to its high surface area and small size, fills the possible pores inside the board  
239 and blocks the water entering the board, thereby reducing the thickness swelling of the board and  
240 increasing the density of the board (Hassanpoor-Tichi *et al.* 2019). Also, with increasing bagasse  
241 content in the boards, their density decreased, which is due to the reversal of the thickness  
242 swelling of the boards made from higher ratios of this lignocellulosic material. The results of  
243 microscopic imaging are a strong reason for this claim (Figure 11). The results indicated that the  
244 fire-retarding properties of the samples were improved by the addition of wollastonite (Figure  
245 10). The lowest mass loss was noted with the sample containing 10 % wollastonite and 15 %  
246 bagasse chip (Figure 10). The reason we can say this is because, firstly, nano-wollastonite has a  
247 high heat transfer (2,5 w/m·K) and its heat is not kept at a single point and is rapidly transferred  
248 to a point where it has less heat and this causes to reduce the fire proofability of boards and  
249 increase their fire resistance (Taghiyari *et al* 2014), secondly, nano-wollastonite contain silica,  
250 titanium, magnesium, calcium and iron that are minerals. This has caused, boards made with  
251 higher amounts of nano-wollastonite have higher relative fire resistance.

252

253

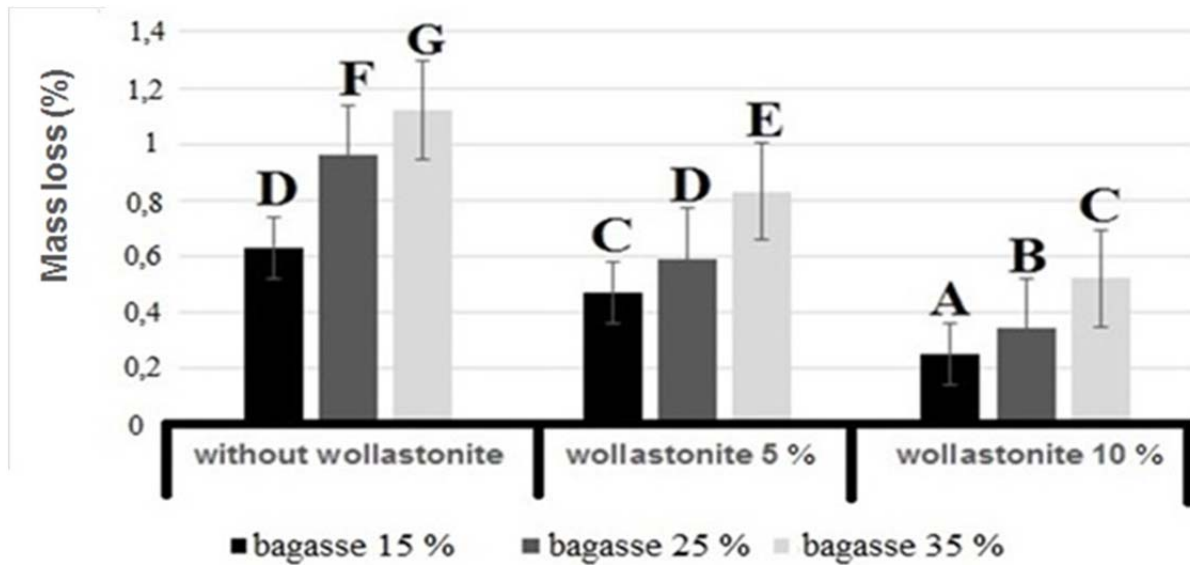


254 **Figure 8:** Effect of varying levels of nano wollastonite on the thickness swelling (TS) of  
 255 composites composed of different percentages of bagasse; letters on each column indicate  
 256 duncan's grouping at the 99 % level of confidence.



257 **Figure 9:** Effect of varying levels of nano wollastonite on density of composites composed of  
 258 different percentages of bagasse; letters on each column indicate duncan's grouping at the 99 %  
 259 level of confidence.

260  
 261  
 262  
 263



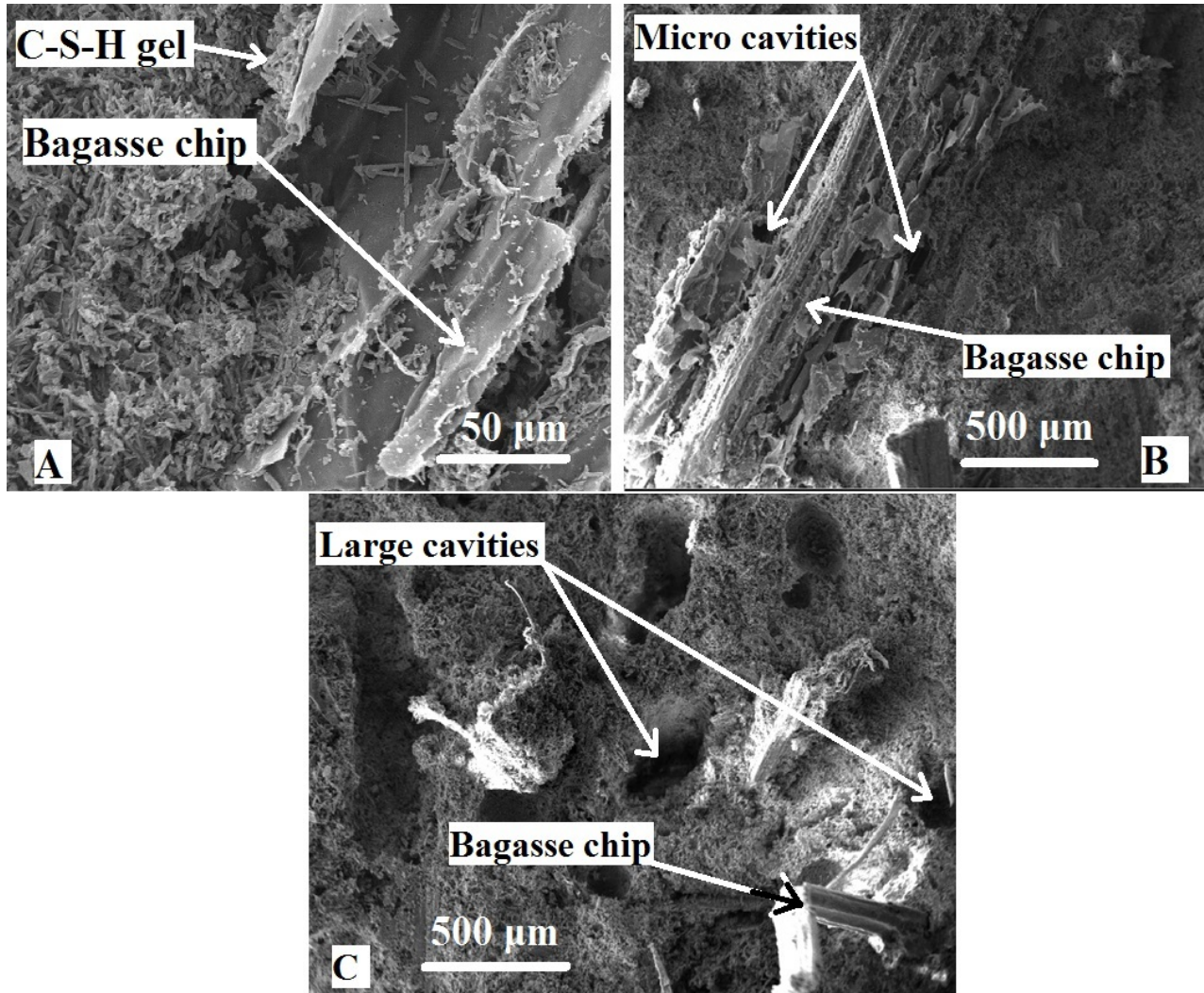
264 **Figure 10:** Effect of varying levels of nano wollastonite on Mass loss of composites composed  
265 of different percentages of bagasse; letters on each column indicate Duncan's grouping at the 99  
266 % level of confidence.

### 267 **Microstructural Investigation**

268 Scanning Electron Microscopy (SEM) was used to investigate the morphology of the fracture  
269 surface of boards. Figure 11 shows different amounts of nano-wollastonite. Increasing nano-  
270 wollastonite from 0 % to 10 % improves the adhesion between bagasse and Gypsum, which can  
271 lead to higher mechanical and physical strength of boards. Also higher percentages of nano-  
272 wollastonite in the boards and reaction of this material with calcium chloride and calcium  
273 hydroxide results in high production of hydrated calcium silicate gel (Figure 11A). This gel  
274 prevents the penetration of chlorine ions, sulfates and other harmful chemicals into the boards  
275 and seals, protects, reduces permeability, durability and self-healing between gypsum and  
276 bagasse. The images also show that nano-wollastonite provides a stronger, provides strong  
277 bonding between bagasse and gypsum, thus filling the porosity and voids between bagasse and  
278 gypsum, thereby increasing the dimensional stability and density of boards. However, as shown



279 in Figure 11A, there is no good bonding between the bagasse chip and the gypsum, and the  
280 absence of nanocrystals causes large cavities.



281 **Figure 11:** Scanning electron microscopy (SEM) of composite Gypsum- bagasse in the presence  
282 of 10 % nano (A), 5 % nano (B) and without- nano (C).

283

### CONCLUSIONS

284 In based on the findings, mechanical strengths of boards such as flexural strength, modulus of  
285 elasticity and internal bonding increased with addition of nano wollastonite content. Increasing  
286 nano wollastonite cause decreases the void, moisture content and increasing of composite  
287 density. Silica in nano-wollastonite forms a calcium silicate hydrate (Ca-Si-H) gel, preventing  
288 the penetration of chlorine ions, sulfates and other harmful chemicals into boards, increasing

289 durability, increasing hydration heat, speeding gypsum and mechanical strength. With the  
290 increase of nano wollastonite, dimensional stability of gypsum board improved. A reason for this  
291 observation could be related to the hydrophobic character of wollastonite. Nano-wollastonite  
292 significantly improved fire-retarding properties in gypsum board. The high thermal conductivity  
293 of wollastonite increased heat transfer, which improved the fire resistance of the composite  
294 boards. Boards made with 15 % bagasse and 10 % nano-wollastonite is recommended to  
295 improve the physical and mechanical properties in gypsum board.

## 296 REFERENCES

- 297 **Ciullo, P.A. 1997.** *Industrial minerals and their uses*. Noyes Publications, Westwood, USA.  
298 640p. [https://www.elsevier.com/books/industrial-minerals-and-their-uses/ciullo/978-0-8155-](https://www.elsevier.com/books/industrial-minerals-and-their-uses/ciullo/978-0-8155-1408-4)  
299 [1408-4](https://www.elsevier.com/books/industrial-minerals-and-their-uses/ciullo/978-0-8155-1408-4)  
300
- 301 **Deutsches Institut für Normung. DIN. 1995.** DIN EN 634-1:1995-04: *Cement-bonded*  
302 *particleboards - Specifications - Part 1: General requirements*. (German version). Berlin,  
303 Germany. <https://dx.doi.org/10.31030/2742430>  
304
- 305 **Deng, Y.H.; Furuno, T. 2001.** Properties of gypsum particleboard reinforced with  
306 polypropylene fibers. *J Wood Sci* 47(6): 445–450. <https://doi.org/10.1007/BF00767896>  
307
- 308 **Dell Inc. 2016.** Dell Statistica, version 13. Data Analysis Software System; Dell Inc., Landolock,  
309 TX, USA.  
310
- 311 **Esmailpour, A.; Taghiyari, H.R.; Nouri, P.; Jahangiri, A. 2017.** Fire-retarding properties of  
312 nano-wollastonite in particleboard. *Fire Mater* 42(6): 306–315. <https://doi.org/10.1002/fam.2493>  
313
- 314 **Espinoza-Herrera. R.; Cloutier. A. 2011.** Physical and mechanical properties of gypsum  
315 particleboard reinforced with Portland cement. *Eur J Wood Wood Prod* 69(2): 247–254.  
316 <https://doi.org/10.1007/s00107-010-0434-x>  
317
- 318 **International Organization for Standardization. ISO. 2010.** EN ISO 11925-2: *Reaction to fire*  
319 *tests – Ignitability of building products subjected to direct impingement of flame – Part 2:*  
320 *Single-flame source test*. ISO, Vernier, Geneva, Switzerland. <https://www.iso.org/>  
321
- 322 **Hassanpoor-Tichi, A.; Bazyar, B.; Khademieslam, H.; Rangavar, H.; Talaeipour, M. 2019.**  
323 *Is Wollastonite Capable of Improving the Properties of Wood Fiber-cement Composite?*  
324 *BioResources* 14(3): 6168-6178. [https://bioresources.cnr.ncsu.edu/resources/is-wollastonite-](https://bioresources.cnr.ncsu.edu/resources/is-wollastonite-capable-of-improving-the-properties-of-wood-fiber-cement-composite/)  
325 [capable-of-improving-the-properties-of-wood-fiber-cement-composite/](https://bioresources.cnr.ncsu.edu/resources/is-wollastonite-capable-of-improving-the-properties-of-wood-fiber-cement-composite/)  
326

- 327 **Haghighi-Poshtiri, A.; Taghiyari, H.R.; Karimi, A.N. 2013.** The optimum level of nano-  
328 wollastonite consumption as fire-retardant in poplar wood (*Populus nigra*). *Int J Nano* 4(2): 141-  
329 151. <http://doi.org/10.7508/ijnd.2013.02.007>
- 330 **Karimi, A.; Haghighi-Poshtiri, A.; Taghiyari, H.R.; Hamzeh, Y.; Enayati, A.A. 2012.**  
331 Effects of nano-wollastonite impregnation on fire resistance and dimensional stability of poplar  
332 wood In *The International Research Group on Wood Protection, IRG/WP 12-40595*. Kuala  
333 Lumpur, Malaysia. [https://www.irg-wp.com//irgdocs/details.php?8a5a2b57-159f-7300-1274-  
334 55d90472351a](https://www.irg-wp.com//irgdocs/details.php?8a5a2b57-159f-7300-1274-55d90472351a)  
335
- 336 **Khosrviyan, B. 2009.** The study of mechanical, physical, thermal and morphological properties  
337 of hybrid multi- structures and nano hybrid polypropylene wood flour/ wollastonite multi-  
338 structures (In Persian). M.S. degree thesis. Department of Natural Resource, The University of  
339 Tehran, Karaj, 103p.
- 340 **Li, H.; Xiao, H.; Ou, J. 2004.** A study on mechanical and pressure-sensitive properties of  
341 cement mortar with nanophase materials. *Cem Concr Res* 34(3): 435-438.  
342 <https://doi.org/10.1016/j.cemconres.2003.08.025>  
343
- 344 **Ma, X.X.; Wang, C.G. 2012.** Hydration characteristics of mixture of grapevine and cement, *J*  
345 *Nanjing For Univ* 36(3): 157-159. (in Chinese) [http://en.cnki.com.cn/Article\\_en/CJFDTotal-  
346 NJLY201203035.htm](http://en.cnki.com.cn/Article_en/CJFDTotal-NJLY201203035.htm)
- 347 **Papadopoulos, A. 2008.** Natural durability and performance of hornbeam cement bonded  
348 particleboard. *Maderas-Cienc Tecnol* 10(2): 93-98. [https://doi.org/10.4067/S0718-  
349 221X2008000200002](https://doi.org/10.4067/S0718-221X2008000200002)
- 350 **Rangavar, H.; Kargarfard, A.; Hoseiny-Fard, M.S. 2016.** Investigation on Effect of cement  
351 types on the cement hydration and properties of wood-cement composites manufactured using  
352 sunflower stalk (*Helianthus Annuus*) (In Persian). *Iran J Wood Paper Sci Res* 31(2): 336-348.  
353 <http://dx.doi.org/10.22092/ijwpr.2016.105933>  
354
- 355 **Taghiyari, H.R.; Mobini, K.; Sarvari- Samadi, Y.; Doosti, Z.; Karimi, F.; Asghari, M.;**  
356 **Jahangiri, A.; Nouri, P. 2013.** Effects of nano-wollastonite on thermal conductivity coefficient  
357 of medium-density fiberboard. *J Nanomater Mol Nanotechnol* 2(1): 1-5.  
358 <http://doi.org/10.4172/2324-8777.1000106>  
359
- 360 **Taghiyari, H.R.; Ghorbanali, M.; Tahir, P.M.D. 2014.** Effects of the improvement in thermal  
361 conductivity coefficient by nano-wollastonite on physical and mechanical properties in medium  
362 density fiberboard (MDF), *BioResources* 9(3): 4138-4149.  
363 <http://doi.org/10.15376/biores.9.3.4138-4149>
- 364 **Yel, H.; Donmez Cavdar. A.; Boran Torun, S. 2020.** Effect of press temperature on some  
365 properties of cement bonded particleboard. *Maderas-Cienc Tecnol* 22(1): 83-92.  
366 <http://doi.org/10.4067/S0718-221X2020005000108>  
367
- 368 **Wei, Y. M.; Tomita, B.; Hiramatsu, Y.; Miyatake, A.; Fujii, T.; Fujii, T.; Yoshinaga, S.**  
369 **2003.** Hydration behavior and compressive strength of cement mixed with exploded wood fiber

370 strand obtained by the water-vapor explosion process. *J Wood Sci* (49): 317-326.  
371 <http://doi.org/10.1007/s10086-002-0479-5>

Accepted manuscript